

## COMPUTATIONAL METHODS FOR EXTREMAL STEKLOV PROBLEMS\*

ELDAR AKHMETGALIYEV<sup>†</sup>, CHIU-YEN KAO<sup>‡</sup>, AND BRAXTON OSTING<sup>§</sup>

**Abstract.** We develop a computational method for extremal Steklov eigenvalue problems and apply it to study the problem of maximizing the  $p$ th Steklov eigenvalue as a function of the domain with a volume constraint. In contrast to the optimal domains for several other extremal Dirichlet- and Neumann-Laplacian eigenvalue problems, computational results suggest that the optimal domains for this problem are very structured. We reach the conjecture that the domain maximizing the  $p$ th Steklov eigenvalue is unique (up to dilations and rigid transformations), has  $p$ -fold symmetry, and has at least one axis of symmetry. The  $p$ th Steklov eigenvalue has multiplicity 2 if  $p$  is even and multiplicity 3 if  $p \geq 3$  is odd.

**Key words.** Steklov eigenvalues, isoperimetric inequality, extremal eigenvalue problems, shape optimization, fluid sloshing

**AMS subject classifications.** 35P15, 49Q10, 65N25

**DOI.** 10.1137/16M1067263

**1. Introduction.** Dedicated to the memory of Russian mathematician Vladimir Andreevich Steklov, a recent article in *Notices of the American Mathematical Society* discuss his remarkable contributions to the development of science [31]. One of his main contributions is on the study of the (second-order) Steklov eigenvalue problem, which has an important application in describing the dynamics of liquid sloshing [37, 27, 6, 32, 30]. Assume that a fluid in a container is inviscid, incompressible, and irrotational and that the surface tension on the free surface is negligible. Denoting the velocity potential by  $\psi(x, y, z)$ , the governing equation for time-harmonic, small-amplitude fluid sloshing is the mixed Steklov eigenvalue problem,

$$(1) \quad \begin{cases} \Delta\psi = 0 & \text{in } W, & \partial_n\psi = \nu\psi & \text{on } F, \\ \partial_n\psi = 0 & \text{on } B, & \text{and} & \int_F \psi ds = 0. \end{cases}$$

Here,  $\Delta$  is the Laplace operator,  $\partial_n$  denotes the normal derivative,  $W \subset \mathbb{R}^3$  is the domain of the liquid,  $F$  is the free surface of the liquid on the top,  $B$  is the wetted rigid part of  $\partial W$ , and  $(\nu, \psi)$  denotes the eigenpair. For sufficiently regular domains, it is known that (1) has a discrete sequence of eigenvalues,  $0 < \nu_1 \leq \nu_2 \leq \nu_3 \leq \dots \rightarrow \infty$ , and corresponding eigenfunctions  $\psi_n \in H^1(W)$ ,  $n = 1, 2, 3, \dots$ . The dominant sloshing behavior corresponds to the smallest eigenfrequency and the high spot (maximal elevation of the free surface) of the corresponding eigenfunction [31]. One of the key questions of interest for the sloshing problem is how to design the container to minimize liquid sloshing, e.g., the sloshing of fuel in a rocket [37].

---

\*Received by the editors March 23, 2016; accepted for publication (in revised form) February 15, 2017; published electronically April 20, 2017.

<http://www.siam.org/journals/sicon/55-2/M106726.html>

**Funding:** The work of the second author was partially supported by NSF grant DMS-1318364. The work of the third author was partially supported by NSF grant DMS-1619755.

<sup>†</sup>Department of Mathematics, Simon Fraser University, Burnaby, BC, Canada (eakhmetg@sfu.edu).

<sup>‡</sup>Department of Mathematical Sciences, Claremont McKenna College, Claremont, CA 91711 (Chiu-Yen.Kao@claremontmckenna.edu).

<sup>§</sup>Department of Mathematics, University of Utah, Salt Lake City, UT 84112 (osting@math.utah.edu).

In this paper, we consider the unmixed Steklov eigenvalue problem,

$$(2) \quad \begin{cases} \Delta u = 0 & \text{in } \Omega, \\ \partial_n u = \lambda u & \text{on } \partial\Omega, \end{cases}$$

where  $\Omega \subset \mathbb{R}^d$  is a bounded open set with Lipschitz boundary  $\partial\Omega$ , and  $(\lambda, u)$  denotes the eigenpair. We view (2) as a simplified model of (1), but it also arises in the study of heat flow and electromagnetics problems. The Steklov spectrum satisfying (2) is also of fundamental interest as it coincides with the spectrum of the Dirichlet-to-Neumann operator  $\Gamma: H^{\frac{1}{2}}(\partial\Omega) \rightarrow H^{-\frac{1}{2}}(\partial\Omega)$ , given by the formula  $\Gamma u = \partial_n(\mathcal{H}u)$ , where  $\mathcal{H}u$  denotes the unique harmonic extension of  $u \in H^{\frac{1}{2}}(\partial\Omega)$  to  $\Omega$ .

The Steklov spectrum is discrete, and we enumerate the eigenvalues in increasing order,  $0 = \lambda_0(\Omega) \leq \lambda_1(\Omega) \leq \lambda_2(\Omega) \leq \dots \rightarrow \infty$ . Weyl’s law for Steklov eigenvalues, the asymptotic rate at which they tend to infinity, is given by  $\lambda_j \sim 2\pi \left(\frac{j}{|\mathbb{B}^{d-1}| |\partial\Omega|}\right)^{\frac{1}{d-1}}$ , where  $\mathbb{B}^{d-1}$  is the unit ball in  $\mathbb{R}^{d-1}$  [22]. The eigenvalues also have a variational characterization,

$$(3) \quad \lambda_k(\Omega) = \min_{v \in H^1(\Omega)} \left\{ \frac{\int_{\Omega} |\nabla v|^2 dx}{\int_{\partial\Omega} v^2 ds} : \int_{\partial\Omega} v u_j ds = 0, j = 0, \dots, k - 1 \right\},$$

where  $u_j$  is the corresponding  $j$ th eigenfunction. It follows from (3) that Steklov eigenvalues satisfy the homothety property  $\lambda_j(t\Omega) = t^{-1}\lambda_j(\Omega)$ . We describe a number of previous results for extremal Steklov problems in section 2.

**Statement of results.** In this short paper, we develop fast and robust computational methods for extremal Steklov eigenvalue problems. We apply these methods to the shape optimization problem

$$(4) \quad \Lambda^{p*} = \max_{\Omega \subset \mathbb{R}^2} \Lambda_p(\Omega), \quad \text{where } \Lambda_p(\Omega) = \lambda_p(\Omega) \cdot \sqrt{|\Omega|}.$$

Note that  $\Lambda_p$  is invariant to dilations, so (4) is equivalent to maximizing  $\lambda_p(\Omega)$  subject to  $|\Omega| = 1$ .

Recently, a general existence result has been established for extremal Steklov eigenvalue problems [8, Theorem 6.4]. In the context of (4), the results are summarized in the following theorem.

**THEOREM 1.1** (see [8]). *The problem  $\max\{\Lambda_p(\Omega) : \Omega \subset \mathbb{R}^2 \text{ open, } \mathcal{H}^1(\partial\Omega) < +\infty\}$  has at least one solution which is bounded and given by the union of at most  $p$  disjoint Jordan domains whose closures intersect pairwise in at most one point. Moreover, every optimal set is bounded and contained in an optimal domain satisfying the previous properties.*

This theorem establishes the existence and some regularity results for the optimal domain. In this paper, we further restrict ourselves to the study of (4) for star-shaped domains. In particular, the assumption that the domains are simply connected is potentially restrictive. In [17] the Steklov eigenvalues on an annulus domain have been computed, and in [22] it was shown that the first Steklov eigenvalue is larger on an annulus domain than on a disk with a fixed perimeter. However, it is still an open question whether one can find a domain with larger Steklov eigenvalues on a non-simply-connected domain with a fixed area.

Our computational studies of (4) for values of  $p$  between 1 and 101 suggest that the optimal domains are very structured and support the following conjecture.

CONJECTURE 1.2. *The maximizer,  $\Omega^{p*}$ , of  $\Lambda_p(\Omega)$  in (4) is unique (up to dilations and rigid transformations), has  $p$ -fold symmetry, and has at least one axis of symmetry. The  $p$ th Steklov eigenvalue has multiplicity 2 if  $p$  is even, and multiplicity 3 if  $p \geq 3$  is odd.*

Furthermore, as described in section 4, the associated eigenspaces are also very structured. This structure stands in stark contrast to previous computational studies for extremal eigenvalue problems involving the Dirichlet- and Neumann-Laplacian spectra. In particular, denoting the Dirichlet- and Neumann-Laplacian eigenvalues of  $\Omega \subset \mathbb{R}^2$  by  $\lambda^D(\Omega)$  and  $\lambda^N(\Omega)$ , respectively, computational results suggest that the optimizers for the following shape optimization problems do not seem to have structure:

$\min_{\Omega \subset \mathbb{R}^2} \lambda_p^D(\Omega) \cdot  \Omega $	[36, 5]
$\min_{\Omega \subset \mathbb{R}^2} (\lambda_p^D(\Omega) + \lambda_{p+1}^D(\Omega)) \cdot  \Omega $	[3]
$\min_{\Omega \subset \mathbb{R}^2} \sum_{p=k}^{k+\ell} c_p \cdot \lambda_p^D(\Omega) \cdot  \Omega $ with $c_p \geq 0$ and $\sum_{p=k}^{k+\ell} c_p = 1$	[34, 35]
$\max_{\Omega \subset \mathbb{R}^2} \frac{\lambda_p^D(\Omega)}{\lambda_1^D(\Omega)}$	[33, 3]
$\min_{\Omega \subset \mathbb{R}^2} \lambda_p^D(\Omega) +  \partial\Omega $	[9, 4]
$\max_{\Omega \subset \mathbb{R}^2} \lambda_p^N(\Omega) \cdot  \Omega $	[5]

The only exception that we are aware of is when the optimal value is attained by a ball or a sequence of domains which degenerates into the disjoint union of balls.

For the problems listed above, we also note that the largest value of  $p$  for which these previous studies have been able to access is  $p \approx 20$ . Here, we compute the optimal domains for  $p = 100$  and  $p = 101$ ; our ability to compute optimal domains for such large values of  $p$  arises from (i) a very efficient and accurate Steklov eigenvalue solver, and (ii) a slight reformulation of the eigenvalue optimization problem that significantly reduces the number of eigenvalue evaluations required.

**Outline.** In section 2, we review some related work. Computational methods are described in section 3. Numerical experiments are presented in section 4, and we conclude in section 5 with a brief discussion.

**2. Related work.** Here we briefly survey some related work; a more comprehensive review can be found in [22] and a historical viewpoint with applications can be found in [31]. Steklov eigenvalues are also discussed in [24], where (4) is given as Open Problem 25.

In 1954, R. Weinstock proved that the disk maximizes the first nontrivial Steklov eigenvalue of

$$(5) \quad \begin{cases} \Delta u = 0 & \text{in } \Omega, \\ \partial_n u = \lambda \rho u & \text{on } \partial\Omega, \end{cases}$$

among *simply connected* planar domains with a fixed total mass  $M(\Omega) = \int_{\partial\Omega} \rho(s) ds$ , where  $\rho$  is an  $L^\infty(\partial\Omega)$  nonnegative weight function on the boundary, referred to as

the “density” [38, 21]. It remains an open question for non-simply-connected bounded planar domains [22]. In 1974, J. Hersch, L. E. Payne, and M. M. Schiffer proved a general isoperimetric inequality for simply connected planar domains which, in a special case, can be expressed as

$$(6) \quad \sup\{\lambda_p(\Omega) \cdot M(\Omega) : \Omega \subset \mathbb{R}^2\} \leq 2\pi p, \quad p \in \mathbb{N}.$$

In [21], Girouard and Polterovich provided an alternative proof based on complex analysis to show that a disk maximizes the first nontrivial Steklov eigenvalue. Furthermore, they proved that the maximum of the second eigenvalue is not attained in the class of simply connected domains, but instead by a sequence of simply connected domains degenerating into a disjoint union of two identical disks. In [20], Girouard and Polterovich proved that the bound in (6) is sharp and attained by a sequence of simply connected domains degenerating into a disjoint union of  $p$  identical balls.

An extension of R. Weinstock’s result to arbitrary Riemannian surfaces  $\Sigma$  with genus  $\gamma$  and  $k$  boundary components was given by Fraser and Schoen in [18]. The inequality

$$(7) \quad \lambda_1(\Sigma) \cdot |\partial\Sigma| \leq 2(\gamma + k)\pi$$

derived therein reduces to Weinstock’s result for  $\gamma = 0$  and  $k = 1$ , and the bound is sharp. However, for  $\gamma = 0$  and  $k = 2$ , the bound is not sharp. See [18] for a better upper bound on annulus surfaces. In [14], it is proven that there exists a constant  $C = C(d)$ , such that for every bounded domain  $\Omega \subset \mathbb{R}^d$ ,

$$(8) \quad \lambda_p(\Omega) \cdot |\partial\Omega|^{\frac{1}{d-1}} \leq Cp^{\frac{2}{d}}, \quad p \geq 1.$$

A generalization for Riemannian manifolds is also given.

Other objective functions depending on Steklov eigenvalues were also considered. In [25], Hersch, Payne, and Schiffer proved that the minimum of  $\sum_{p=1}^n \lambda_p^{-1}(\Omega)$  is attained when  $\Omega$  is a disk for both perimeter and area constraints. This result is generalized to arbitrary dimensions in [12]. In [17], it is proven that sums of squared reciprocal Steklov eigenvalues,  $\sum_{p=1}^{\infty} \lambda_p^{-2}(\Omega)$ , for simply connected domains with a fixed perimeter are minimized by a disk. Sharp isoperimetric upper bounds have been found for the sum of the first  $p$  eigenvalues, partial sums of the spectral zeta function, and the heat trace for starlike and simply connected domains using quasi-conformal mappings to a disk [19].

There are also a few computational studies of extremal Steklov problems. The most relevant is recent work of Bogosel [7], which is primarily concerned with the development of methods based on fundamental solutions to compute the Steklov, Wentzell, and Laplace–Beltrami eigenvalues. This method was used to demonstrate that the ball is the minimizer for a variety of shape optimization problems. The author also studies the problem of maximizing the first five Wentzell eigenvalues subject to a volume constraint, for which (4) is a special case. Shape optimization problems for Steklov eigenvalues with mixed boundary conditions have also been studied [10].

### 3. Computational methods.

**3.1. Computation of Steklov eigenvalues.** We consider the Steklov eigenvalue problem (2) where the domain  $\Omega$  is simply connected with smooth boundary  $\partial\Omega$ . Without loss of generality we assume that  $\partial\Omega$  possesses a  $2\pi$ -periodic counterclockwise parametric representation of the form

$$x(t) = (x_1(t), x_2(t)), \quad 0 \leq t \leq 2\pi.$$

Use of integral equation methods for (2) leads directly upon discretization to a matrix eigenvalue problem [26, 13]. In order to avoid the inclusion of hypersingular operators we use eigenfunction representations based on a single-layer potential. The eigenfunction  $u(x)$  is represented using a single-layer potential,  $\varphi$ , with a slight modification to ensure uniqueness of the solution:

$$(9) \quad u(x) = \frac{S_0[\varphi]}{2} = \int_{\partial\Omega} \Phi(x-y)(\varphi(y) - \bar{\varphi})ds(y) + \bar{\varphi},$$

where  $\Phi(x) = \frac{1}{2\pi} \log|x|$  and  $\bar{\varphi} = \frac{1}{|\partial\Omega|} \int_{\partial\Omega} \varphi(y)ds(y)$ . The boundary operator  $S_0 : C^{0,\alpha}(\partial\Omega) \rightarrow C^{1,\alpha}(\partial\Omega)$  is bijective; see [29, Theorem 7.41]. Taking into account well-known expressions (see, e.g., [29]) for the jump of the single-layer potential and its normal derivative across  $\partial\Omega$ , the eigenvalue problem (2) reduces to the integral eigenvalue equation for  $(\lambda, \varphi)$ ,

$$(10) \quad A[\varphi] = \lambda B[\varphi].$$

Here, the boundary operators  $A$  and  $B$  are defined as

$$A[\varphi](x) := \int_{\partial\Omega} \frac{\partial\Phi(x-y)}{\partial n(x)} (\varphi(y) - \bar{\varphi})ds(y) + \frac{1}{2}(\varphi(x) - \bar{\varphi}),$$

$$B[\varphi](x) := \lambda \left( \int_{\partial\Omega} \Phi(x-y)(\varphi(y) - \bar{\varphi})ds(y) + \bar{\varphi} \right).$$

In the cases considered in this paper, the Steklov eigenfunctions  $u_k$  and the corresponding densities  $\varphi_k$  are smooth functions. These problems can thus be treated using highly effective spectrally accurate methods [15, 29] based on explicit resolution of logarithmic singularities and a Fourier series approximation of the density. To construct a spectral method for approximation of the integral operators in (10), we use an explicit  $2\pi$ -parametrization of the boundary  $\partial\Omega$ . The periodic parametric domain is discretized using an  $n$ -point uniform grid. The density  $\varphi$  and smooth integrands in the approximated integral operators (10) are represented in a Fourier basis and integrated with spectral accuracy. For the logarithmic integration, Nyström quadratures are used, which also yields spectral accuracy; see [29]. This spectrally accurate approximation of the integral equation system results in a generalized matrix eigenvalue problem of the form

$$(11) \quad \mathbf{AX} = \mathbf{LBX},$$

which can be solved numerically by means of the QZ-algorithm (see [23]). More details about this method can be found in [1, 2].

In Figure 1, we demonstrate the spectral convergence of this boundary integral method. In the left panel we depict a domain that was obtained as an optimizer for the 50th Steklov eigenvalue. In polar coordinates, this domain is given by  $\{(r, \theta) : r < R(\theta)\}$ , where

$$R(\theta) = 2.5 + 0.057475351612645 \cdot \cos(50 \theta) + 0.002675998736772 \cdot \cos(100 \theta) \\ - 0.002569287572637 \cdot \cos(150 \theta).$$

In the right panel, we display a log-log convergence plot of the first 100 Steklov eigenvalues of the domain shown in the left panel, as we increase the number  $n$  of interpolation points. For ground-truth, we used  $n = 1800$ .

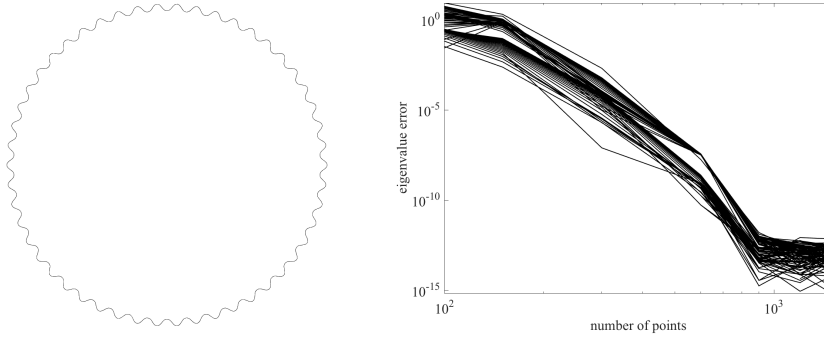


FIG. 1. A log-log convergence plot of the first 100 eigenvalues for the domain on the left as the number of interpolation points increases.

**3.2. Eigenvalue perturbation formula.** The following proposition gives the Steklov eigenvalue perturbation formula, which can also be found in [16].

PROPOSITION 3.1. Consider the perturbation  $x \mapsto x + \tau v$  and write  $c = v \cdot \hat{n}$ , where  $\hat{n}$  is the outward unit normal vector. Then a simple (unit-normalized) Steklov eigenpair  $(\lambda, u)$  satisfies the perturbation formula

$$(12) \quad \lambda' = \int_{\partial\Omega} (|\nabla u|^2 - 2\lambda^2 u^2 - \lambda \kappa u^2) c \, ds.$$

*Proof.* Let primes denote the shape derivative. From the identity  $\lambda = \int_{\Omega} |\nabla u|^2 \, dx$ , we compute

$$\begin{aligned} \lambda' &= 2 \int_{\Omega} \nabla u \cdot \nabla u' \, dx + \int_{\partial\Omega} |\nabla u|^2 c \, ds && \text{(shape derivative)} \\ &= -2 \int_{\Omega} (\Delta u) u' \, dx + 2 \int_{\partial\Omega} u_n u' \, ds + \int_{\partial\Omega} |\nabla u|^2 c \, ds && \text{(Green's identity)} \\ &= 2\lambda \int_{\partial\Omega} uu' \, ds + \int_{\partial\Omega} |\nabla u|^2 c \, ds && \text{(equation (2)).} \end{aligned}$$

Differentiating the normalization equation,  $\int_{\partial\Omega} u^2 \, ds = 1$ , we have that

$$\int_{\partial\Omega} uu' \, ds = - \int_{\partial\Omega} \left( uu_n + \frac{\kappa}{2} u^2 \right) c \, ds = - \int_{\partial\Omega} \left( \lambda + \frac{\kappa}{2} \right) u^2 c \, ds.$$

Putting these two equations together, we obtain (12). □

**3.3. Shape parameterization.** We consider domains of the form

$$(13) \quad \Omega = \{(r, \theta) : 0 \leq r < \rho(\theta)\}, \quad \text{where } \rho(\theta) = \sum_{k=0}^m a_k \cos(k\theta) + \sum_{k=1}^m b_k \sin(k\theta).$$

The velocities corresponding to a perturbation of the  $k$ th cosine and sine coefficients are given by

$$\frac{\partial \mathbf{x}(\theta)}{\partial a_k} \cdot \hat{n}(\theta) = \frac{\rho(\theta) \cos(k\theta)}{\sqrt{\rho^2(\theta) + [\rho'(\theta)]^2}} \quad \text{and} \quad \frac{\partial \mathbf{x}(\theta)}{\partial b_k} \cdot \hat{n}(\theta) = \frac{\rho(\theta) \sin(k\theta)}{\sqrt{\rho^2(\theta) + [\rho'(\theta)]^2}}.$$

The derivative of Steklov eigenvalues with respect to Fourier coefficients can be obtained using Proposition 3.1.

**3.4. Optimization method.** We apply gradient-based optimization methods to minimize spectral functions of Steklov eigenvalues, such as (4). The gradient of a simple eigenvalue is provided in Proposition 3.1. While Steklov eigenvalues are not differentiable when they have multiplicity greater than one, in practice, eigenvalues computed numerically that approximate the Steklov eigenvalues of a domain are generically simple. Thus, we are faced with the problem of maximizing a function that we know to be nonsmooth, but whose gradient is well-defined at generic points we sample.

To compute solutions to the eigenvalue optimization problem (4), we (trivially) reformulate the problem as a minimax problem,

$$\max_{\Omega \subset \mathbb{R}^2} \min_{j: p \leq j \leq p-1+m} \Lambda_j(\Omega), \quad m \geq 1.$$

This minimax problem can be numerically solved by first reformulating as

$$\begin{aligned} & \max_{\Omega \subset \mathbb{R}^2} t \\ & \text{s.t. } \Lambda_j(\Omega) \geq t, \quad j = p, p+1, \dots, p-1+m, \end{aligned}$$

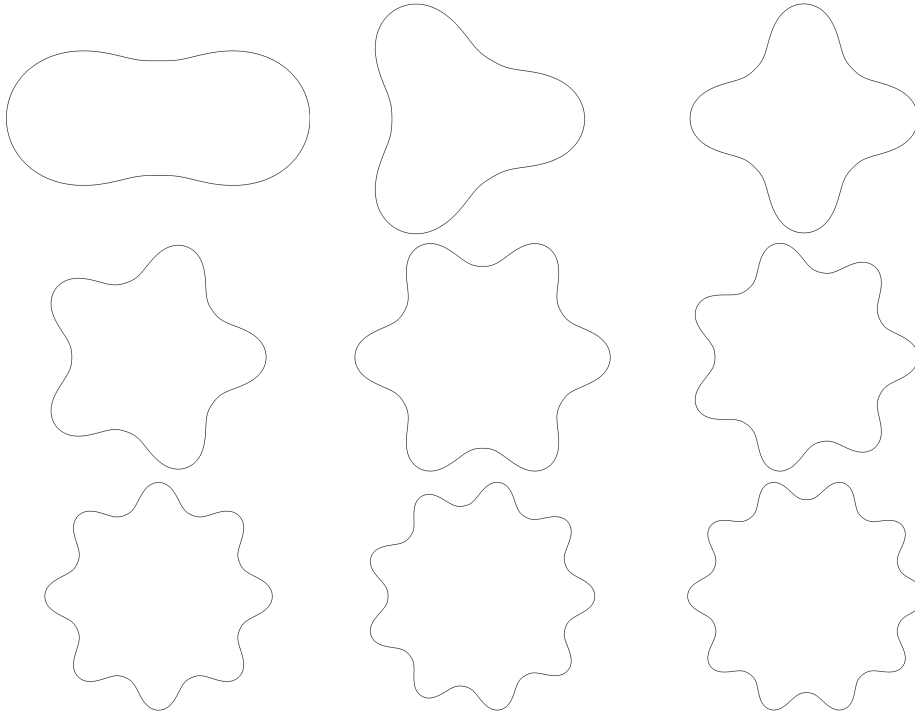
and using a sequential quadratic programming (SQP) method [11], as implemented in the MATLAB function `fminimax`. We use as convergence criteria a tolerance on either the relative change on stepsize or function value. We choose  $m$  to exceed the (expected) multiplicity of the eigenvalue at the optimal solution. For (4), we find this method to be more effective than using the BFGS quasi-Newton method directly, as reported in other computational studies of extremal eigenvalues [33, 5, 34, 35, 28].

**4. Numerical results.** In this section, we apply the computational methods developed in section 3 to the Steklov eigenvalue optimization problem (4). The methods are implemented in MATLAB, and numerical results are obtained on a 4-core 4GHz Intel Core i7 computer with 32GB of RAM. Unless specified otherwise, we initialize with randomly chosen Fourier coefficients, and the number of interpolation points used is  $6 \cdot p \cdot m$ , where  $p$  is the eigenvalue considered and  $m$  is the largest free Fourier coefficient for the domain.

**Initial results.** Optimal domains,  $\Omega^{p^*}$ , for  $\Lambda^{p^*}$  for  $p = 2, \dots, 10$  are plotted in Figure 2. We also define  $\Lambda_j^{p^*} := \Lambda_j(\Omega^{p^*})$  and tabulate  $\Lambda_j^{p^*}$  for  $j = 1, \dots, 12$ . In Figures 3 and 4, we plot the eigenfunctions corresponding to  $\Lambda_j^{p^*}$  for  $j = p-1, p, p+1$  if  $p$  is even, and  $j = p, p+1, p+2$  if  $p \geq 3$  is odd. The eigenfunctions are extended outside of  $\Omega^{p^*}$  using the representation (9). The optimal domains and their eigenpairs are very structured. Namely, for these values of  $p$ , we make the following (numerical) observations:

1. The optimal domains,  $\Omega^{p^*}$ , are unique (up to dilations and rigid transformations).
2.  $\Omega^{p^*}$  looks like a “ruffled pie dish” with  $p$  “ruffles” where the curvature of the boundary is positive. In particular,  $\Omega^{p^*}$  has  $p$ -fold rotational symmetry and an axis of symmetry.
3. The  $p$ th eigenvalue has multiplicity 2 for  $p$  even and multiplicity 3 for  $p \geq 3$  odd, i.e.,

$$\begin{aligned} p \text{ even: } & \Lambda_p^{p^*} = \Lambda_{p+1}^{p^*} < \Lambda_{p+2}^{p^*}, \\ p \text{ odd: } & \Lambda_p^{p^*} = \Lambda_{p+1}^{p^*} = \Lambda_{p+2}^{p^*} < \Lambda_{p+3}^{p^*}. \end{aligned}$$



$j/p$	1	2	3	4	5
1	<b>1.77245385087</b>	0.77711553416	1.08009419126	1.17184143852	1.23983446877
2	<b>1.77245385087</b>	<b>2.91607062996</b>	1.08009419126	1.17184143852	1.23983446877
3	3.54489505800	<b>2.91607062996</b>	<b>4.14530094752</b>	1.61218026073	1.94641573795
4	3.54492034560	3.27779066969	<b>4.14530094753</b>	<b>5.28443697870</b>	1.94641573795
5	5.31736077095	4.49874762429	<b>4.14530094753</b>	<b>5.28443697870</b>	<b>6.49648330968</b>
6	5.31736233451	5.04108010599	4.91549057961	5.44835286940	<b>6.49648330968</b>
7	7.08981538184	6.11836168338	6.02473863720	5.44835286940	<b>6.49648330968</b>
8	7.08981542529	6.27292391406	6.02473863720	6.49307907483	6.73220322361
9	8.86226925401	7.69339202998	7.62864589136	7.33722449947	6.73220322361
10	8.86226925490	7.81074114281	7.62864589136	7.33722449947	8.13365983464
11	10.63472310534	9.26310835729	8.95411656010	8.63569850900	8.80703776153
12	10.63472310535	9.30894713716	9.13942771171	9.03967498150	8.80703776153

$j/p$	6	7	8	9	10
1	1.26679073258	1.29332099645	1.30507111512	1.31877096745	1.32527400403
2	1.26679073258	1.29332099645	1.30507111512	1.31877096745	1.32527400403
3	2.12087896619	2.25492147182	2.33230070074	2.40062714807	2.44325807518
4	2.12087896619	2.25492147182	2.33230070074	2.40062714807	2.44325807518
5	2.43137356740	2.78418204027	3.00802851250	3.18864047723	3.30989719981
6	<b>7.64509491772</b>	2.78418204027	3.00802851250	3.18864047723	3.30989719981
7	<b>7.64509491772</b>	<b>8.84784433682</b>	3.24728287256	3.61129280434	3.86836939850
8	7.77206522336	<b>8.84784433682</b>	<b>10.00272938023</b>	3.61129280434	3.86836939850
9	7.77206522336	<b>8.84784433682</b>	<b>10.00272938023</b>	<b>11.20007255719</b>	4.06278154050
10	7.97924507207	9.05209069188	10.10344300189	<b>11.20007255719</b>	<b>12.35895460691</b>
11	7.97924507207	9.05209069188	10.10344300189	<b>11.20007255719</b>	<b>12.35895460692</b>
12	9.73604655977	9.22612069487	10.32907157080	11.37140333632	12.44176614187

FIG. 2. (Top)  $\Omega^{p*}$  for  $p = 2, \dots, 10$ . The optimal domain for  $p = 1$  is a ball. (Bottom) Values  $\Lambda_j(\Omega^{p*})$  for  $p = 1, \dots, 10$  and  $j = 1, \dots, 12$ . See section 4.

4. There is a very large gap between  $\Lambda_{p-1}^{p*}$  and  $\Lambda_p^{p*}$ . For even  $p$ ,  $\Lambda_{p-1}^{p*}$  is simple.
5. For even  $p$ , the eigenfunction corresponding to  $\Lambda_{p-1}$  (left) and two eigenfunctions from the eigenspace corresponding to  $\Lambda_p = \Lambda_{p+1}$  (center and right) are plotted in Figure 3. The eigenfunctions are all nearly zero at the center of the

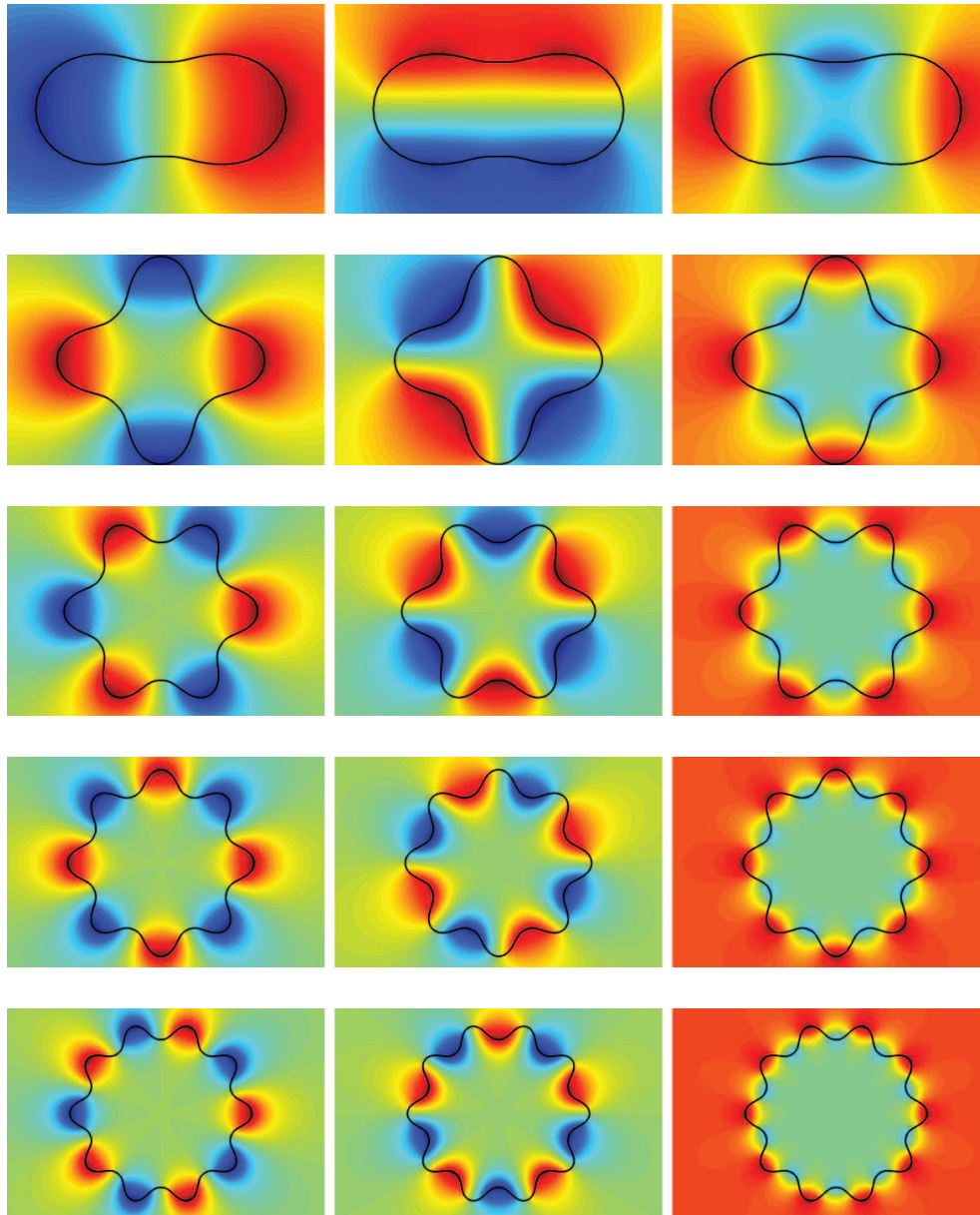


FIG. 3. For  $\Omega^{p*}$  with even  $p = 2, 4, 6, 8, 10$ , Steklov eigenfunctions  $p - 1$ ,  $p$ , and  $p + 1$ . Here,  $\Lambda_{p-1} < \Lambda_p = \Lambda_{p+1} < \Lambda_{p+2}$ .

domain and oscillatory on the boundary. The eigenfunction corresponding to  $\Lambda_{p-1}$  takes alternating maxima and minima on the “ruffles” of the domain. Eigenfunctions from the  $\Lambda_p = \Lambda_{p+1}$  eigenspace may be chosen so that one eigenfunction is nearly zero on the “ruffles” of the domain and takes alternating maxima and minima in between. The other eigenfunction takes maxima on the “ruffles” of the domain and minima in between.

For odd  $p \geq 3$ , in Figure 4 we plot the eigenfunctions from the three-

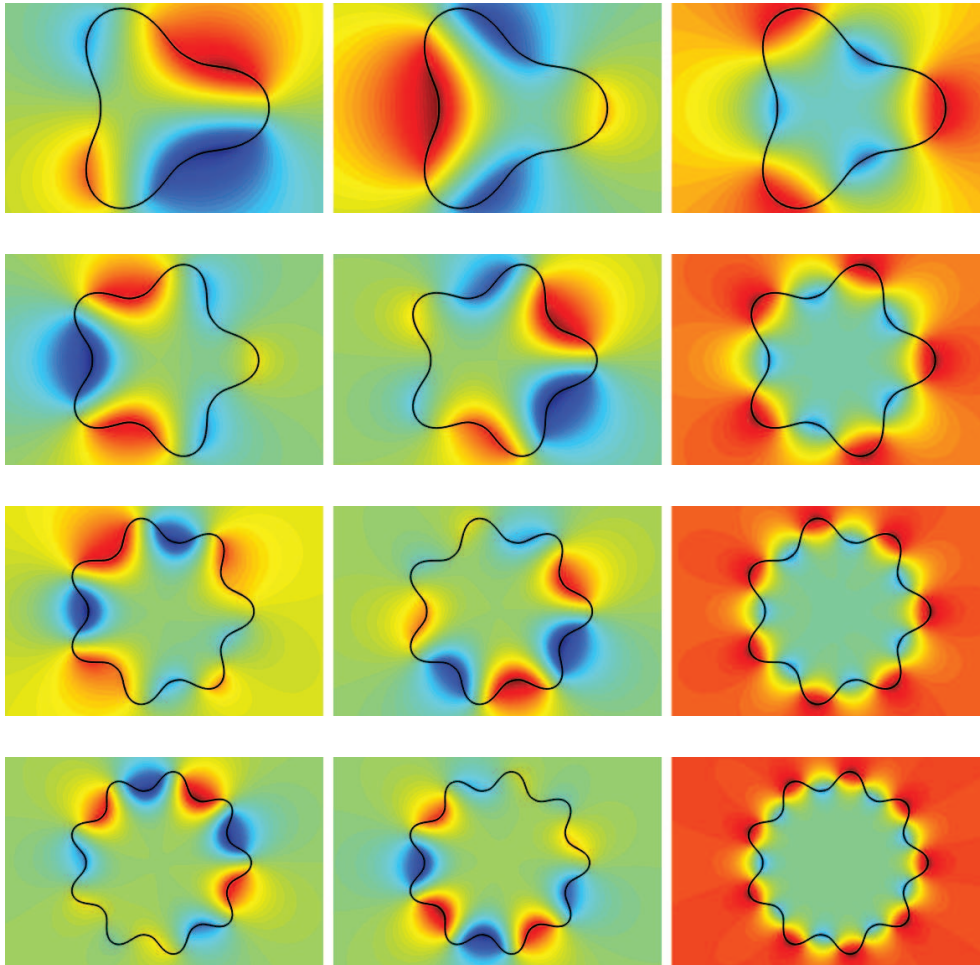


FIG. 4. For  $\Omega^{p*}$  with odd  $p = 3, 5, 7, 9$ , Steklov eigenfunctions  $p, p + 1$ , and  $p + 2$ . Here,  $\Lambda_{p-1} < \Lambda_p = \Lambda_{p+1} = \Lambda_{p+2} < \Lambda_{p+3}$ .

dimensional eigenspace corresponding to  $\Lambda_p = \Lambda_{p+1} = \Lambda_{p+2}$ . Again, eigenfunctions from this subspace are nearly zero on the interior of the domain and oscillatory on the boundary. They may be chosen so that, again, one eigenfunction takes maxima on the “ruffles” of the domain and minima in between (right figures). The other two eigenfunctions are nearly zero on the “ruffles” of the domain and take alternating maxima and minima in between on the boundary. These two eigenfunctions are concentrated on opposite sides of the domain.

Some of these observations are also summarized in Conjecture 1.2. For  $p = 2, 3, 4, 5$ , the domain symmetries have also been observed in the recent numerical results of Bogosel [7]. Preliminary results indicate that the introduction of a hole in the domain decreases the  $p$ th eigenvalue. To consider larger values of  $p$ , we use the structure of the optimal domains for relatively small  $p$  to reduce the search space and generate good initial domains for the optimization procedure.

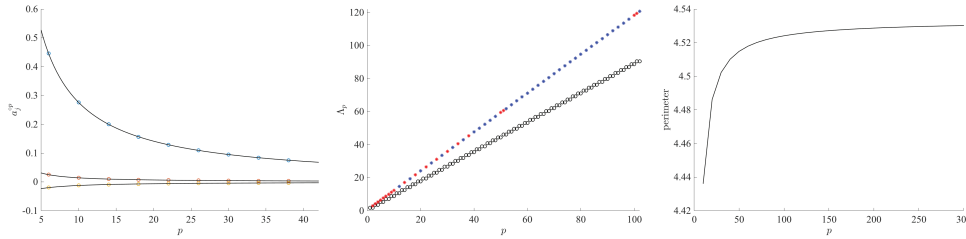


FIG. 5. (Left) For  $p = 6, 10, 14, \dots, 38$ , a plot of the coefficients  $a_{k,p}^{p^*}$  for  $k = 1, 2, 3$  and the interpolation in (14). (Center) Value of  $\Lambda_p$  for a ball (black), interpolated domains  $\Omega^{p^\circ}$  (blue), and optimal domains  $\Omega^{p^*}$  (red). The values for  $\Omega^{p^\circ}$  and  $\Omega^{p^*}$  are indistinguishable. (Right) The perimeter of  $\Omega^{p^\circ}$  as a function of  $p$ .

**Structured coefficients.** If a domain has  $p$ -fold symmetry, the only nonzero coefficients in the Fourier expansion (13) are multiples of  $p$ . If there is an axis of symmetry, then we can further assume  $b_k = 0$  for  $k \geq 1$ . Therefore, since we observe that the optimal domains have  $p$ -fold symmetry and an axis of symmetry, when minimizing the  $p$ th eigenvalue, we only vary the coefficients  $a_{k,p}$  for  $k = 1, 2, \dots, K$ . This simplification reduces the shape optimization problem to an optimization problem with just  $K$  parameters. For values  $p \leq 10$  we can use, say,  $K = 10$  coefficients (corresponding to multiples of  $p$ ) and obtain the same optimal values as obtained by including nonmultiple coefficients. For larger values of  $p$ , using this many coefficients is computationally infeasible. For values  $p \leq 10$ , we also used  $K = 3$  coefficients to compute optimal domains. Of course, in this case, the optimal values are slightly smaller but the optimal domains are very similar and, in particular, the all observed properties (described above) of the eigenvalues/functions still hold. To explore optimal domains for very large values of  $p$ , we therefore use only  $K = 3$  coefficients (corresponding to multiples of  $p$ ).

Let  $\{a_j^{p^*}\}_j$  denote the coefficients corresponding to  $\Omega^{p^*}$ . Solving (4) for  $p \leq 40$ , we observe that, as a function of  $p$ , the coefficients  $\{a_{k,p}^{p^*}\}_{k=1,2,3}$  decay at a rate  $a_{k,p}^{p^*} \propto \frac{1}{p}$ . Using computed values for the optimal coefficients, we obtain the following interpolations, denoted  $\{a_j^{p^\circ}\}_j$ :

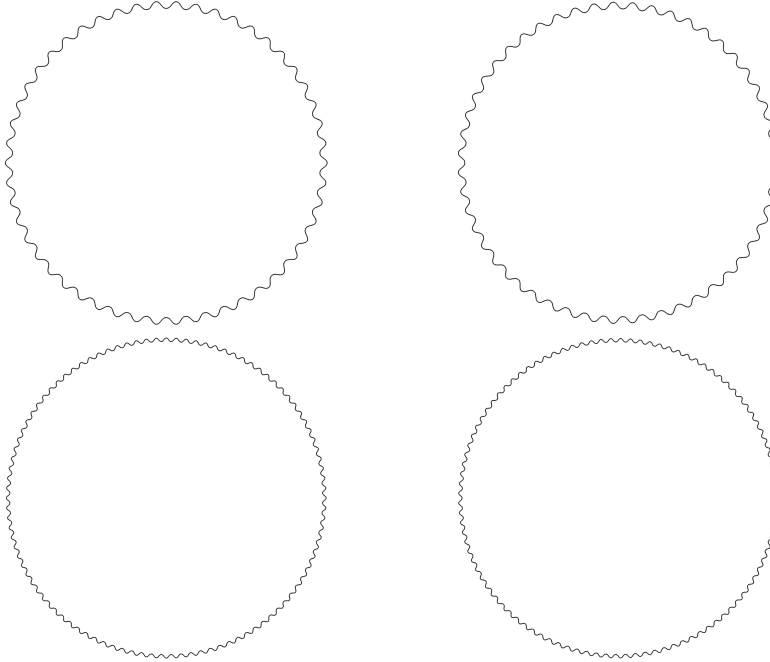
$$(14) \quad \begin{aligned} a_{0,p}^{p^\circ} &= 2.5, & a_{1,p}^{p^\circ} &= \frac{1}{0.1815 + 0.3444 \cdot p}, & a_{2,p}^{p^\circ} &= \frac{1}{-6.1198 + 7.6443 \cdot p}, \\ a_{3,p}^{p^\circ} &= \frac{1}{-4.5563 - 7.6561 \cdot p}. \end{aligned}$$

A plot of these three interpolations is given in Figure 5 (left). Let  $\Omega^{p^\circ}$  denote the domain corresponding to these coefficients,  $\{a_j^{p^\circ}\}_j$ . In Figure 5 (center), we plot  $\Lambda_p(\Omega^{p^\circ})$  in blue,  $\Lambda_p(\Omega^{p^*})$  in red, and the value of  $\Lambda_p$  for a ball in black. The values for  $\Omega^{p^\circ}$  and  $\Omega^{p^*}$  are indistinguishable, although the multiplicity of the  $p$ th eigenvalue for these two domains differs. We observe that the value of  $\Lambda_p(\Omega^{p^\circ})$  grows linearly with  $p$ . Linear interpolation of  $\Lambda_p(\Omega^{p^\circ})$  gives

$$(15) \quad \Lambda_p(\Omega^{p^\circ}) \approx 0.5801 + 1.1765 \cdot p.$$

Linear interpolation of the eigenvalues of a ball gives

$$\Lambda_p(\mathbb{B}) \approx 0.4436 + 0.8862 \cdot p.$$



j/p	50	51	100	101
$p - 2$	20.30936391721	20.75355064378	40.69488836617	41.11849978908
$p - 1$	20.34992971509	20.75355064378	40.71526210762	41.11849978908
$p$	<b>59.41361758262</b>	<b>60.59374478101</b>	<b>118.23330554334</b>	<b>119.41159188027</b>
$p + 1$	<b>59.41361758262</b>	<b>60.59374478101</b>	<b>118.23330554339</b>	<b>119.41159188027</b>
$p + 2$	59.43099705171	<b>60.59374478101</b>	118.24200985153	<b>119.41159188027</b>
$p + 3$	59.43099705171	60.62775851108	118.24200985153	119.42881860937
$p + 4$	59.48272776444	60.62775851108	118.26807069001	119.42881860937

FIG. 6. (Top)  $\Omega^{p*}$  for  $p = 50, 51, 100, 101$ . (Bottom) Values  $\Lambda_j(\Omega^{p*})$  for  $j = p - 2, \dots, p + 4$ .

The interpolation for a ball is in good agreement with Weyl’s law,  $\lambda_j(\Omega)|\partial\Omega| \sim j\pi$ , since for a ball we have  $|\partial\Omega| = 2\sqrt{\pi}|\Omega|^{\frac{1}{2}}$  and

$$\Lambda_p(\mathbb{B}^2) = \lambda_p(\mathbb{B}^2)\sqrt{|\mathbb{B}^2|} = \frac{1}{2\sqrt{\pi}}\lambda_p(\mathbb{B}^2)|\partial\mathbb{B}^2| \sim \frac{\sqrt{\pi}}{2} \cdot p.$$

One can view (15) in terms of the bound given in (8). In dimension two, using the isoperimetric inequality,  $4\pi|\Omega| \leq |\partial\Omega|^2$ , we have that

$$\Lambda_p(\Omega) = \lambda_p(\Omega) \cdot |\Omega|^{\frac{1}{2}} \leq \frac{1}{2\sqrt{\pi}}\lambda_p(\Omega) \cdot |\partial\Omega| \leq \tilde{C}p.$$

We have constructed a sequence of domains with maximal value  $\Lambda_p(\Omega)$  and so have computed the (optimal) value of  $\tilde{C}$  in this inequality. For the interpolated domains,  $\Omega^{p^\circ}$ , we plot  $p$  vs. the perimeter,  $|\partial\Omega^{p^\circ}|/\sqrt{|\Omega^{p^\circ}|}$ , in Figure 5 (right). We observe that the perimeter appears to converge to a value near 4.53, which is greater than the value for the disc,  $2\sqrt{\pi} \approx 3.54$ .

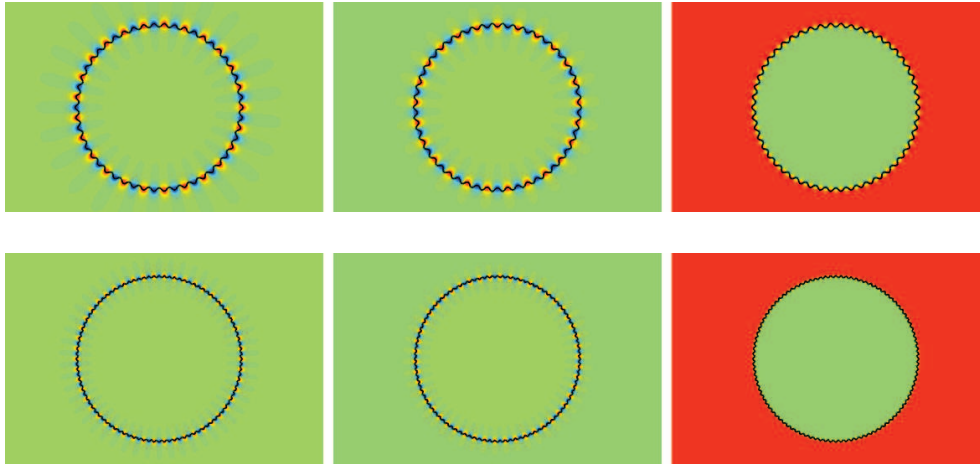


FIG. 7.  $p - 1$ ,  $p$ , and  $p + 1$  Steklov eigenfunctions of  $\Omega^{p^*}$  for  $p = 50$  (top) and  $p = 100$  (bottom).

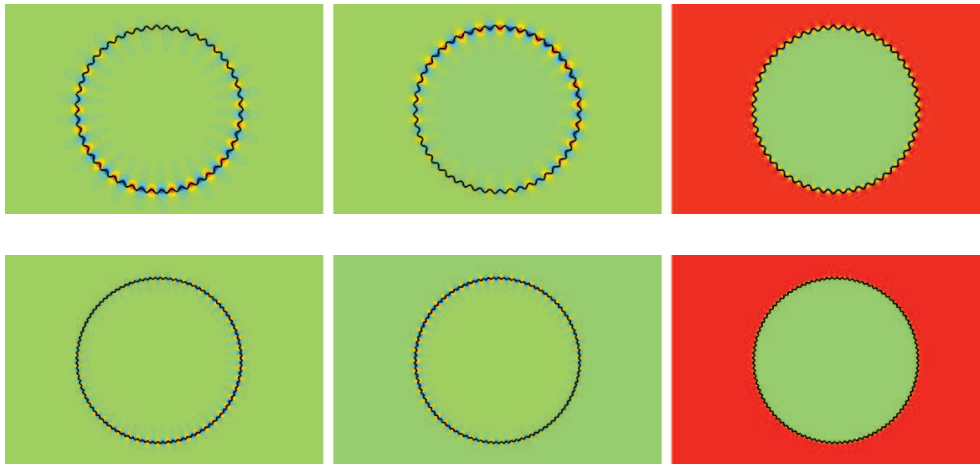


FIG. 8.  $p$ ,  $p + 1$ , and  $p + 2$  Steklov eigenfunctions of  $\Omega^{p^*}$  for  $p = 51$  (top) and  $p = 101$  (bottom).

**Solution of (4) for large  $p$ .** We extrapolate the interpolation given in (14) to  $p = 50, 51, 100, 101$ . Using this as an initial condition for the optimization problem (4), where we restrict the admissible set to domains with coefficients  $a_{k,p}$  for  $k = 1, 2, 3$ , we solve the optimization problem to obtain domains,  $\Omega^{p^*}$ , plotted in Figure 6. Here, we also tabulate  $\Lambda_j^{p^*}$  for  $j = p - 2, \dots, p + 4$ . In Figures 7 and 8, we plot the eigenfunctions corresponding to  $\Lambda_j^{p^*}$  for  $j = p - 1, p, p + 1$  if  $p$  is even, and  $j = p, p + 1, p + 2$  if  $p$  is odd. The observations made above for small values of  $p$  hold here as well.

**5. Discussion.** In this paper, we developed a computational method for extremal Steklov eigenvalue problems and applied it to study the problem of maximizing the  $p$ th Steklov eigenvalue as a function of the domain with a volume constraint. The optimal domains, spectrum, and eigenfunctions are very structured, in contrast with other extremal eigenvalue problems. There are several interesting directions for this work. The first is to use conformal or quasi-conformal maps to better understand the optimal domains (see [19]). It would be very interesting to extend these computational

results to higher dimensions and see if the optimal domains there are also structured. The computational methods developed here could also be used to investigate other functions of the Steklov spectrum. Finally, the optimal domains in this work could potentially find application in sloshing problems, where it is desirable to engineer a vessel to have a large spectral gap to avoid certain exciting frequencies [37].

**Acknowledgments.** We would like to thank Dorin Bucur for pointing us towards [16], and Oscar Bruno and Nilima Nigam for collaboration in building the eigenvalue solver.

## REFERENCES

- [1] E. AKHMETGALIYEV, *Fast Numerical Methods for Mixed, Singular Helmholtz Boundary Value Problems and Laplace Eigenvalue Problems—with Applications to Antenna Design, Sloshing, Electromagnetic Scattering and Spectral Geometry*, Ph.D. thesis, California Institute of Technology, Pasadena, CA, 2016.
- [2] E. AKHMETGALIYEV, O. BRUNO, N. NIGAM, AND N. TAZHIMBETOV, *A high-accuracy boundary integral strategy for the Steklov eigenvalue problem*, 2016.
- [3] P. R. S. ANTUNES, *Optimization of sums and quotients of Dirichlet–Laplacian eigenvalues*, Appl. Math. Comput., 219 (2013), pp. 4239–4254, <https://doi.org/10.1016/j.amc.2012.10.095>.
- [4] P. R. S. ANTUNES AND P. FREITAS, *Optimisation of eigenvalues of the Dirichlet Laplacian with a surface area restriction*, Appl. Math. Optim., 73 (2016), pp. 313–328, <https://doi.org/10.1007/s00245-015-9304-6>.
- [5] P. R. S. ANTUNES AND P. FREITAS, *Numerical optimization of low eigenvalues of the Dirichlet and Neumann Laplacians*, J. Optim. Theory Appl., 154 (2012), pp. 235–257, <https://doi.org/10.1007/s10957-011-9983-3>.
- [6] R. BANUELOS, T. KULCZYCKI, I. POLTEROVICH, AND B. SIUDEJA, *Eigenvalue inequalities for mixed Steklov problems*, in Operator Theory and Its Applications, Amer. Math. Soc. Transl. Ser. 2 231, AMS, Providence, RI, 2010, pp. 19–34, <https://doi.org/10.1090/trans2/231/04>.
- [7] B. BOGOSEL, *The method of fundamental solutions applied to boundary eigenvalue problems*, J. Comput. Appl. Math., 306 (2016), pp. 265–285, <https://doi.org/10.1016/j.cam.2016.04.008>.
- [8] B. BOGOSEL, D. BUCUR, AND A. GIACOMINI, *Optimal Shapes Maximizing the Steklov Eigenvalues*, preprint, <http://www.math.ens.fr/~bogospel/pdfs/BBG-submitted.pdf>.
- [9] B. BOGOSEL AND É. OUDET, *Qualitative and numerical analysis of a spectral problem with perimeter constraint*, SIAM J. Control Optim., 54 (2016), pp. 317–340, <https://doi.org/10.1137/140999530>.
- [10] J. F. BONDER, P. GROISMAN, AND J. D. ROSSI, *Optimization of the first Steklov eigenvalue in domains with holes: A shape derivative approach*, Ann. Mat. Pura Appl. (4), 186 (2007), pp. 341–358, <https://doi.org/10.1007/s10231-006-0009-y>.
- [11] R. BRAYTON, S. DIRECTOR, G. HACHTEL, AND L. VIDIGAL, *A new algorithm for statistical circuit design based on quasi-Newton methods and function splitting*, IEEE Trans. Circuits Syst., 26 (1979), pp. 784–794, <https://doi.org/10.1109/tcs.1979.1084701>.
- [12] F. BROCK, *An isoperimetric inequality for eigenvalues of the Stekloff problem*, ZAMM Z. Angew. Math. Mech., 81 (2001), pp. 69–71.
- [13] P. CHENG, J. HUANG, AND Z. WANG, *Nyström methods and extrapolation for solving Steklov eigensolutions and its application in elasticity*, Numer. Methods Partial Differential Equations, 28 (2012), pp. 2021–2040, <https://doi.org/10.1002/num.21695>.
- [14] B. COLBOIS, A. EL SOUFI, AND A. GIROUARD, *Isoperimetric control of the Steklov spectrum*, J. Funct. Anal., 261 (2011), pp. 1384–1399, <https://doi.org/10.1016/j.jfa.2011.05.006>.
- [15] D. L. COLTON AND R. KRESS, *Inverse Acoustic and Electromagnetic Scattering Theory*, Springer, New York, 1998, <https://doi.org/10.1007/978-1-4614-4942-3>.
- [16] M. DAMBRINE, D. KATEB, AND J. LAMBOLEY, *An extremal eigenvalue problem for the Wentzell–Laplace operator*, Ann. Inst. H. Poincaré Anal. Non Linéaire, 33 (2016), pp. 409–450, <https://doi.org/10.1016/j.anihpc.2014.11.002>.
- [17] B. DITTMAR, *Sums of reciprocal Stekloff eigenvalues*, Math. Nachr., 268 (2004), pp. 44–49, <https://doi.org/10.1002/mana.200310158>.
- [18] A. FRASER AND R. SCHOEN, *The first Steklov eigenvalue, conformal geometry, and minimal surfaces*, Adv. Math., 226 (2011), pp. 4011–4030, <https://doi.org/10.1016/j.aim.2010.11.007>.

- [19] A. GIROUARD, R. S. LAUGESSEN, AND B. A. SIUDEJA, *Steklov eigenvalues and quasiconformal maps of simply connected planar domains*, Arch. Ration. Mech. Anal., 219 (2016), pp. 903–936, <https://doi.org/10.1007/s00205-015-0912-8>.
- [20] A. GIROUARD AND I. POLTEROVICH, *On the Hersch-Payne-Schiffer inequalities for Steklov eigenvalues*, Funct. Anal. Appl., 44 (2010), pp. 106–117, <https://doi.org/10.1007/s10688-010-0014-1>.
- [21] A. GIROUARD AND I. POLTEROVICH, *Shape optimization for low Neumann and Steklov eigenvalues*, Math. Methods Appl. Sci., 33 (2010), pp. 501–516, <https://doi.org/10.1002/mma.1222>.
- [22] A. GIROUARD AND I. POLTEROVICH, *Spectral Geometry of the Steklov Problem*, preprint, <https://arxiv.org/abs/1411.6567>, 2014.
- [23] G. H. GOLUB AND C. F. VAN LOAN, *Matrix Computations*, 4th ed., Johns Hopkins University Press, Baltimore, MD, 2013.
- [24] A. HENROT, *Extremum Problems for Eigenvalues of Elliptic Operators*, Springer, New York, 2006, <https://doi.org/10.1007/3-7643-7706-2>.
- [25] J. HERSCH, L. E. PAYNE, AND M. M. SCHIFFER, *Some inequalities for Stekloff eigenvalues*, Arch. Ration. Mech. Anal., 57 (1974), pp. 99–114, <https://doi.org/10.1007/bf00248412>.
- [26] J. HUANG AND T. LÜ, *The mechanical quadrature methods and their extrapolation for solving BIE of Steklov eigenvalue problems*, J. Comput. Math., 22 (2004), pp. 719–726.
- [27] R. A. IBRAHIM, *Liquid Sloshing Dynamics: Theory and Applications*, Cambridge University Press, Cambridge, UK, 2005, <https://doi.org/10.1017/cbo9780511536656>.
- [28] C.-Y. KAO, R. LAI, AND B. OSTING, *Maximization Laplace-Beltrami eigenvalues on closed Riemannian surfaces*, ESAIM Control Optim. Calc. Var., 23 (2017), pp. 685–720, <https://doi.org/10.1051/cocv/2016008>.
- [29] R. KRESS, *Linear Integral Equations*, Appl. Math. Sci. 82, Springer, New York, 1999, <https://doi.org/10.1007/978-1-4612-0559-3>.
- [30] T. KULCZYCKI, M. KWAŚNICKI, AND B. SIUDEJA, *The shape of the fundamental sloshing mode in axisymmetric containers*, J. Engrg. Math., (2014), pp. 1–27, <https://doi.org/10.1007/s10665-015-9826-6>.
- [31] N. KUZNETSOV, T. KULCZYCKI, M. KWAŚNICKI, A. NAZAROV, S. POBORCHI, I. POLTEROVICH, AND B. SIUDEJA, *The legacy of Vladimir Andreevich Steklov*, Notices Amer. Math. Soc., 61 (2014), pp. 9–22, <https://doi.org/10.1090/noti1073>.
- [32] H. MAYER AND R. KRECHETNIKOV, *Walking with coffee: Why does it spill?*, Phys. Rev. E, 85 (2012), 046117, <https://doi.org/10.1103/physreve.85.046117>.
- [33] B. OSTING, *Optimization of spectral functions of Dirichlet-Laplacian eigenvalues*, J. Comput. Phys., 229 (2010), pp. 8578–8590, <https://doi.org/10.1016/j.jcp.2010.07.040>.
- [34] B. OSTING AND C.-Y. KAO, *Minimal convex combinations of sequential Laplace-Dirichlet eigenvalues*, SIAM J. Sci. Comput., 35 (2013), pp. B731–B750, <https://doi.org/10.1137/120881865>.
- [35] B. OSTING AND C.-Y. KAO, *Minimal convex combinations of three sequential Laplace-Dirichlet eigenvalues*, Appl. Math. Optim., 69 (2014), pp. 123–139, <https://doi.org/10.1007/s00245-013-9219-z>.
- [36] E. OUDET, *Numerical minimization of eigenmodes of a membrane with respect to the domain*, ESAIM Control Optim. Calc. Var., 10 (2004), pp. 315–330, <https://doi.org/10.1051/cocv:2004011>.
- [37] B. A. TROESCH, *An isoperimetric sloshing problem*, Comm. Pure Appl. Math., 18 (1965), pp. 319–338, <https://doi.org/10.1002/cpa.3160180124>.
- [38] R. WEINSTOCK, *Inequalities for a classical eigenvalue problem*, J. Rational Mech. Anal., 3 (1954), pp. 745–753, <https://doi.org/10.1512/iumj.1954.3.53036>.